BDX-613-1706

SOLDERABILITY TEST DEVELOPMENT

PDO 6989288, Final Report

D. M. Jarboe, Project Leader

Project Team:
R. L. Comstock
R. A. Wilson

Published October 1977

Prepared for the United States Energy Research and Development Administration Under Contract Number EY-76-C-04-0613 USERDA

Bendix Kansas City Division

DISCLAIMER

NOTICE

Printed in the United States of America

Available From the National Technical Information Service, U.S. Department of Commerce, 5285 Port Royal Road, Springfield, Virginia 22161.

Price: Microfiche $2.25
Paper Copy $4.~~00~~ 50

BDX-613-1706
Distribution Category UC-38

SOLDERABILITY TEST DEVELOPMENT

Published October 1977

Project Leader:
D. M. Jarboe
Department 814

Project Team:
R. L. Comstock
R. A. Wilson

PDO 6989288
Final Report

Communications Services Bendix Kansas City Division

SOLDERABILITY TEST DEVELOPMENT

BDX-613-1706, UNCLASSIFIED Final Report, Published October 1977

Prepared by D. M. Jarboe, D/814, under PDO 6989288

Operating procedures and data reduction techniques applicable to a General Electric Company, Limited, Meniscograph were developed. The information provides a means of directly correlating solderability with the physical phenomenon of wetting.

WPC-bap

The Bendix Corporation
Kansas City Division
P.O. Box 1159
Kansas City, Missouri 64141

A prime contractor with the United States Energy Research and Development Administration under Contract Number EY-76-C-04-0613 USERDA

CONTENTS

ILLUSTRATIONS

TABLES

SUMMARY

Operating procedures and data reduction techniques applicable to the Meniscograph (General Electric Company, Limited) were developed. Using force-time traces from tests involving various sample materials and configurations, flux types, and test temperatures, the wetting rate and contact angle were obtained through statistical treatment of the data. This information provides a means of directly correlating solderability with the physical phenomenon of wetting.

DISCUSSION

SCOPE AND PURPOSE

The purpose of this study (PDO 6989288) was to develop operating procedures and data reduction techniques for the Meniscograph solderability tester (CE47198) recently acquired by Bendix Kansas City. To accomplish this, solderability tests were to be performed on various materials commonly soldered at Bendix.

PRIOR WORK

The Meniscograph solderability tester is being used at both Sandia Albuquerque and Sandia Livermore. A significant step in the analysis of Meniscograph data was made by applying statistical techniques to aid in interpretation.[1] This work was partly used as a basis for the development of the Meniscograph testing and analysis study under this process development order.

ACTIVITY

Equipment and Raw Data Output

The Meniscograph (Figure 1) operates on the same principle employed in the Wilhemy slide method[2] of liquid surface tension measurement. A specimen is inserted a small distance into the liquid--in this case solder--and the resulting force on the specimen as wetting proceeds is measured. The Meniscograph minimizes the possibility for human error during actual testing by applying automation. The specimen and its holder are suspended from a linear variable differential transformer (LVDT) load cell. The output of the LVDT is manually adjusted to zero thereby nullifying the weight of the specimen and holder. As the test is initiated, the temperature controlled solder pot rapidly raises until electrical contact is made to the specimen (Figure 2). Controlled overrun of the electric jack raising the solder pot results in immersion of the specimen into the molten solder. The actual immersion depth can be preset to 1, 2, 3, or 5 mm.

As the solder wets the specimen, a meniscus is formed above the surface of the solder. Since the meniscus is supported by the specimen, a downward force is produced on the specimen which is equal to the weight of the solder in the meniscus. This phenomenon is explained by a brief discussion of the classical physics of wetting. Figure 3 shows the point at which the solder, flux, and specimen meet. The interfaces between these three materials exhibit a surface energy or tension as represented by the arrows.

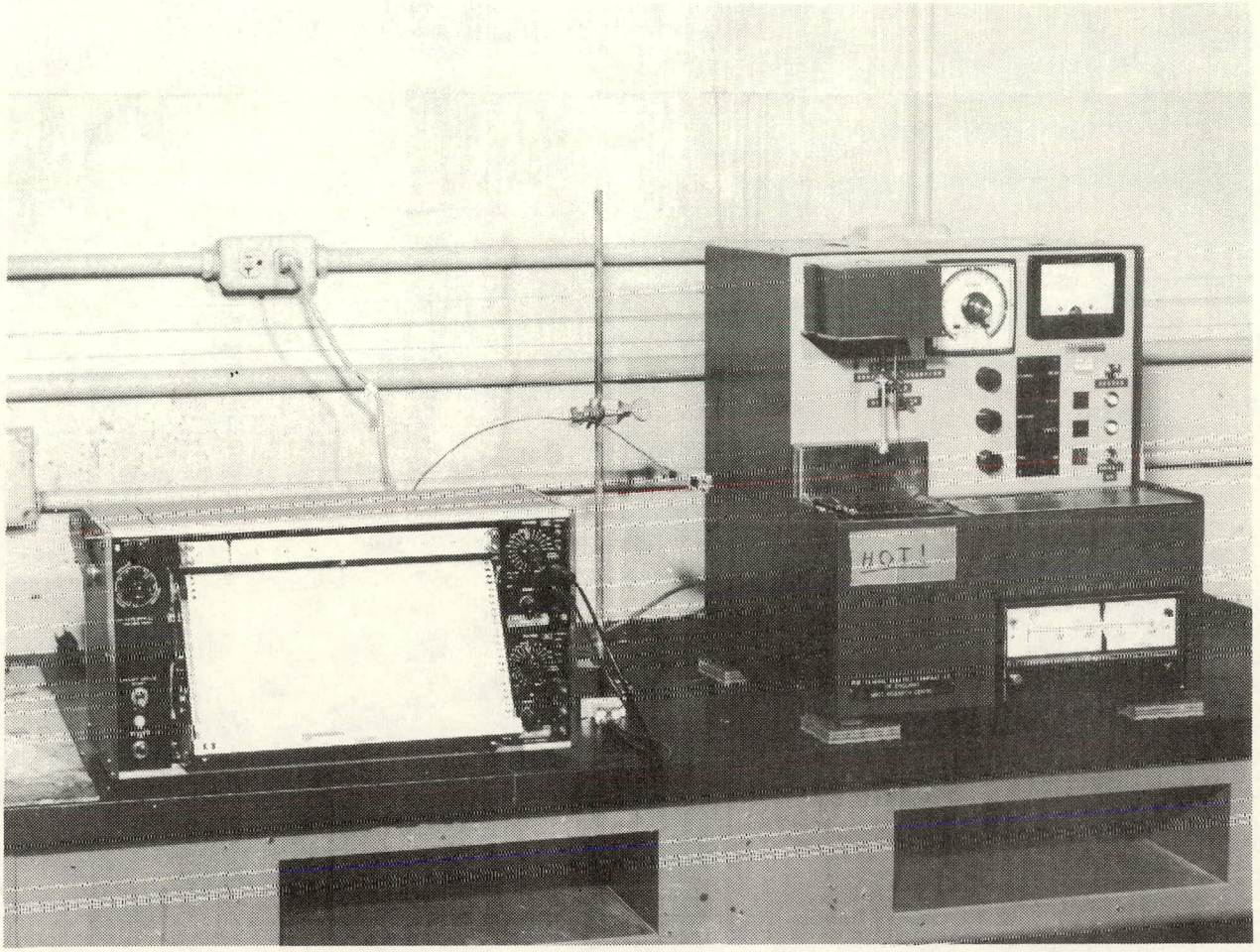

Figure 1. Meniscograph Solderability Tester

At the point where all three meet, a force balance exists at equilibrium such that

$$\gamma_{sf} = \gamma_{sl} + \gamma_{lf}\cos\theta,$$

where

γ_{sf} = the surface tension at the solder-flux interface,

γ_{sl} = the surface tension at the solder-liquid interface,

γ_{lf} = the surface tension at the liquid flux interface, and

θ = contact angle.

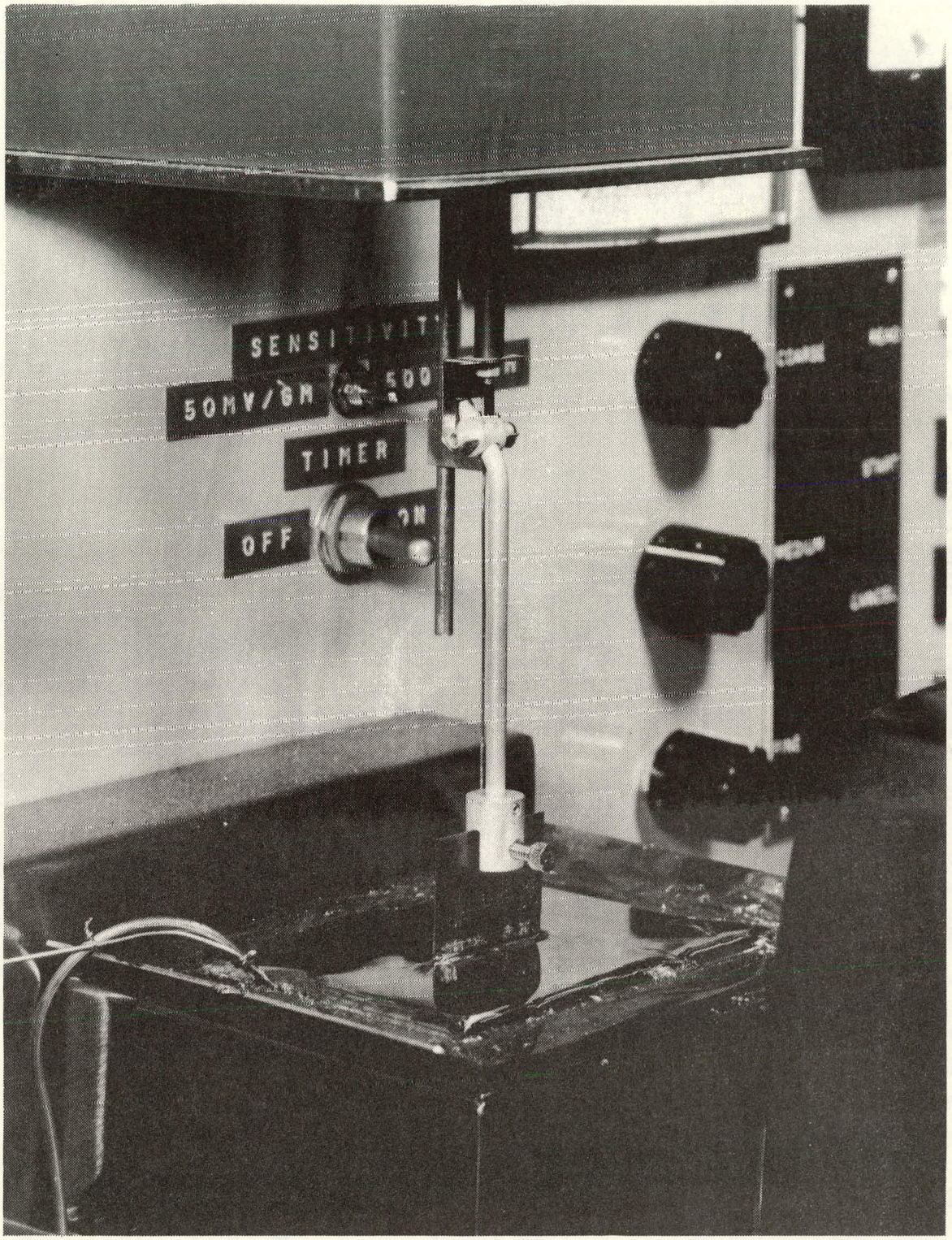

Figure 2. Sample With Holder Supported by LVDT at the Beginning of Testing

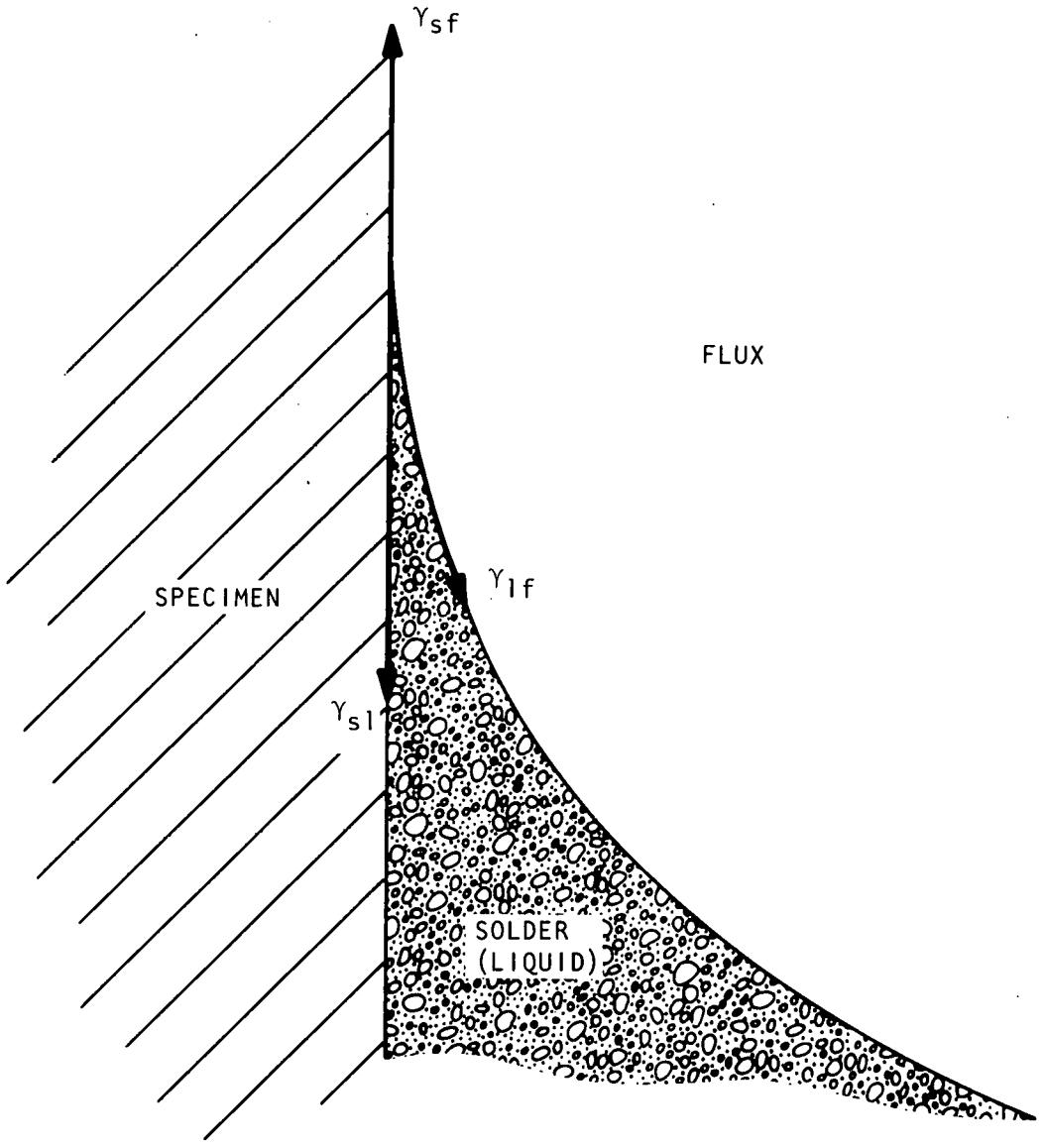

Figure 3. Surface Tension Interaction in the Solder-Flux Specimen System

The force (σ), measured by the Meniscograph, is the factor $\gamma_{lf}\cos\theta$.

Therefore, this force is affected by the surface tension γ_{lf} and the contact angle (θ).

This wetting force is converted to a dc voltage by the LVDT and is used to drive a Hewlett Packard Model 7100B strip chart recorder. Two output voltage ranges are provided in the Meniscograph. The ranges are 5.1 V/N (50 mV/gmf) and 51 V/N (500 mV/gmf). This provides a force-time record of the wetting process during the test.

A timer is used to preset the duration of the test up to 10 seconds. Actual timing begins when the sample contacts the solder.

Prior to solderability testing, two modifications were made to the Meniscograph. First, a switch was installed which would disenable the timer thereby permitting test durations in excess of 10 seconds. This was done to allow the testing of samples which exhibited low wetting rates and would not reach an equilibrium wetting force value within 10 seconds. The second modification was the installation of a switch to allow better LVDT output voltage range switching. Otherwise, this operation would have required some disassembly of the Meniscograph to change internal electrical connections.

As mentioned previously, the output of this testing system is a force-time trace from the strip chart recorder. Figure 4 is such a trace. Before a test is initiated, the strip chart is zeroed at midscale. When the solder contacts the specimen (point A) an initial negative spike is obtained (point A to point B) due to buoyancy of the sample in the molten solder and a downward or negative meniscus. As wetting beings, the meniscus rises and the chart pen crosses over the null line (point C) and reaches equilibrium (point D). At the end of the test the solder pot is lowered resulting in a spike (point E).

Test Variables and Sample Preparation

The solder used throughout this study was Sn63 (63Sn/37Pb). Meniscograph solderability tests were performed on seven different specimen types using three fluxes and three test temperatures (Table 1).

It was initially planned that each copper and nickel specimen should be chemically cleaned and artificially oxidized before testing. Preliminary attempts at this, however, were not considered suitable due to the lack of uniformity among samples after oxidizing, so it was decided to use all samples in the as-received condition. This was felt to be acceptable since the copper did exhibit a uniform natural tarnish and the nickel had aged naturally in the laboratory for about 3 years. Upon further consideration, it was concluded that these sample conditions were preferable since the surfaces consisted of other compounds such as sulfides and carbonates which would be present in an actual aged condition.

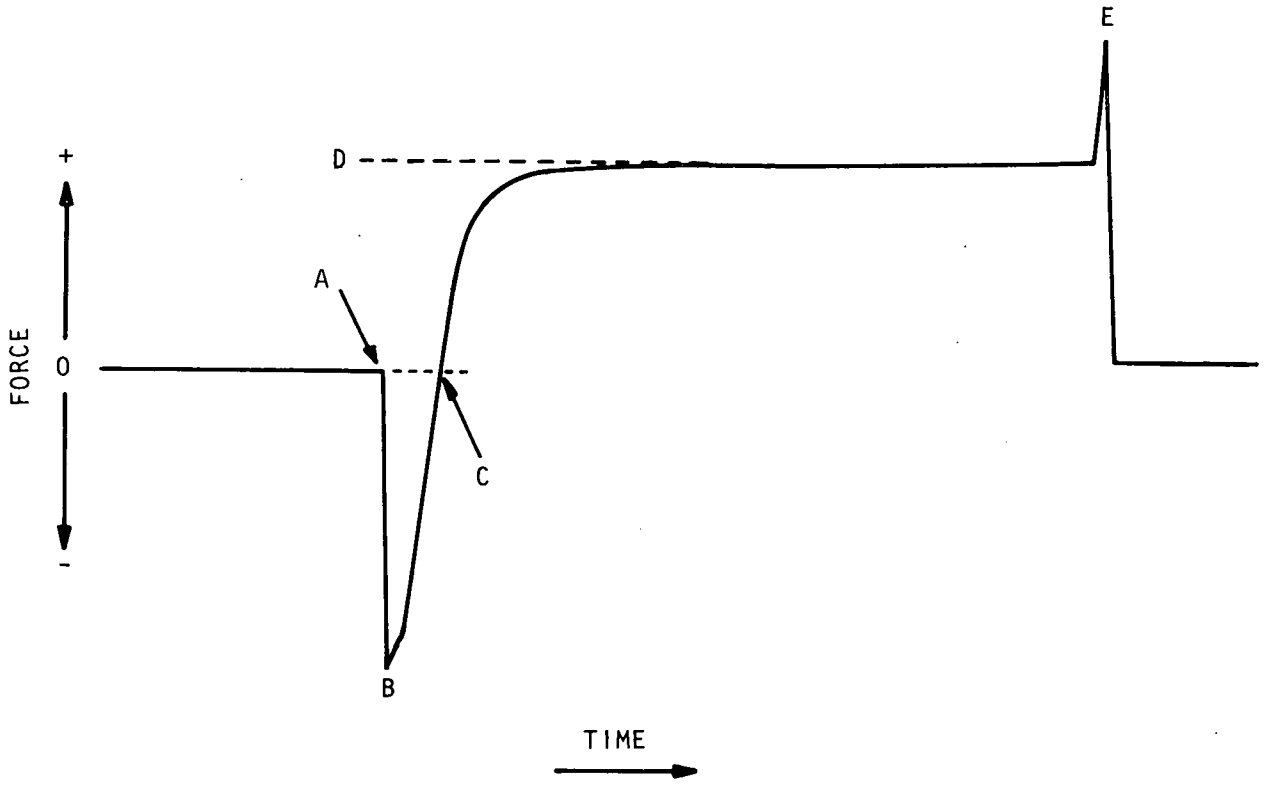

Figure 4. Trace of a Meniscograph Solderability Test

Data Analysis Techniques

When the Meniscograph method of solderability testing was first developed, interpretation consisted of measuring the time for the trace to cross the null line (A to C in Figure 4) and the maximum indicated wetting force above the null line. Subsequent investigations have found that these two measurements are not always consistent.[1,3] As a result, statistical techniques for characterizing the trace have been developed which provide the desired coherence in the data.[1]

Before any data reduction can be performed, however, two preliminary steps must be taken to utilize the force-time trace. First, a starting point on the trace must be determined. This has been selected as the force correlating to the time at which the contact angle θ is equal to 90 degrees. This value was selected for two reasons. First, a previous study concluded that there may be substantial errors in the force-time trace when the contact angle is greater than 90 degrees.[1] Second, at the point that θ equals 90 degrees, the wetting force (σ) has no input to the load cell. This can be quickly seen by visualizing an angle

Table 1. Meniscograph Test Variables of 63 Groups

Sample	Flux	Test Temperature (°C)
Copper Sheet*	Alpha 100, Type R	232
Nickel Sheet**	Kester 197, Type RMA	260
Gold Plated Copper Sheet†	Kester 1544, Type RA	287
Copper Sheet**		
Nickel Sheet		
Copper Wire***		
Tinned Copper Wire††		

*25.4 by 25.4 by 0.25 mm (1 by 1 by 0.01 in.)
**25.4 by 25.4 by 0.56 mm (1 by 1 by 0.02 in.)
***0.76 mm diameter (0.03 in.)
†Copper coupons were plated with nickel (5 μm or 200 μin.) or gold (1.3 μm or 50 μin.)
††Wires were pretinned in Sn63 solder.

of 90 degrees in Figure 3. Since the specimen is not supporting a meniscus, the only force detected by the load cell is a buoyancy force equal to $\rho \cdot V$, where ρ is the density of the solder at test temperature and V is the immersed volume of the specimen. The buoyancy force is then located on the chart as shown in Figure 5. This point serves as the zero wetting force and zero time for all subsequent operations. The second step to be taken is the conversion of the force in grams to surface energy units of $mN \cdot m/m^2$ (mN/m). This is done by first multiplying the force in grams by the factor 9.80665 mN/g. The resulting value is then divided by the specimen perimeter (or circumference) in centimeters. For example, a wetting force of 1 gram on a sample measuring 25.4 by 25.4 by 2.54 mm, tested on edge (Figure 2), would be found to convert to a surface tension of 175.49 mN/m.

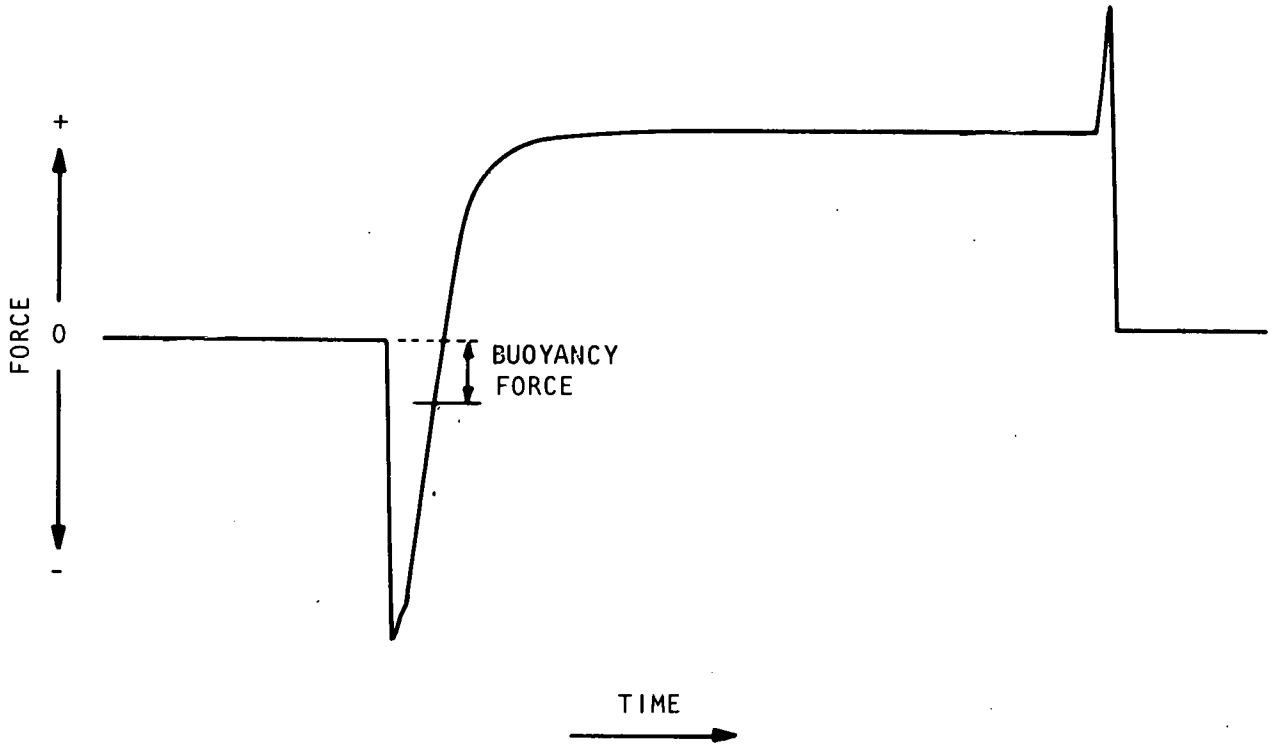

Figure 5. Selection of Zero Wetting Force

The most promising method of data reduction developed by Jellison[1] is the use of a plot of the function

$$\ln \frac{\sigma_{max}-\sigma}{\sigma_{max}} \quad \text{versus time}$$

where σ_{max} is the final equilibrium wetting force and

σ is the time dependent wetting force.

This results in a straight line which can be determined by regression analysis. The slope of this line (having units of sec^{-1}) has been found to be a good measure of wetting rate. This technique was pursued further in this study using the following formulations.

Assuming

$$\ln \frac{\sigma_{max}-\sigma}{\sigma_{max}} = At+B,$$

where

A is the slope and

B is the intercept as determined by regression analysis,

then

$$\frac{\sigma_{max}-\sigma}{\sigma_{max}} = \exp(At+B)$$

which yields

$$\sigma = \sigma_{max}\ 1-\exp(At+B).$$

Differentiating with respect to time,

$$\frac{d\sigma}{dt} = -A\sigma_{max}\exp(At+B) \text{ (units of dynes/cm/sec).} \qquad 1.$$

This expression can be simplified by considering the boundary condition at $t = 0$. Since by definition $\sigma = 0$ at this point, it can be shown that $B = 0$.

Thus

$$\frac{d\sigma}{dt} = -A\sigma_{max}\exp(At). \qquad 2.$$

In production situations the wetting rate is most important at $t = 0$ which results in the equation,

$$\frac{d\sigma}{dt} = -A\sigma_{max}. \qquad 3.$$

In addition to the use of Equation 3 in determining information about the kinetics of the wetting process, the wetting rate can also be used to determine activation energies for wetting.[4]

By plotting

$$\ln \frac{d\sigma}{dt} \text{ versus } \frac{1}{T},$$

where T is the test temperature in Kelvins, a straight line is obtained.

The slope of this line is equal to the quantity

$$\frac{-\Delta H_a}{R},$$

where

ΔH_a = the activation energy and

R = the universal gas constant

$$8.31 \frac{J}{mol\ K} \text{ or } 1.987 \frac{cal}{mol\ K}.$$

This type of analysis, although not particularly useful in normal production oriented testing or quality control, would provide useful information when new soldering processes and materials are being investigated.

Wetting rate data alone do not provide a complete picture of solderability. Some measure of the extent or degree of wetting is also necessary. A particular part under test may, for example, show a very high initial wetting rate, but still exhibit a large contact angle.

Two methods are used to determine the degree of wetting. The first, based on the classical physics of wetting, involves the use of an equation describing the shape of the meniscus, termed the elastica[3]

$$1-\sin\theta = g \frac{\rho_L-\rho_F}{\gamma_{LF}} \frac{Y^2}{2}, \qquad 4.$$

where

g = acceleration due to gravity,

ρ_L = density of the liquid solder at temperature = 8000 kg/m^3,

ρ_F = density of the liquid flux at temperature = 1000 kg/m^3,

γ_{LF} = surface tension at interface between the solder and

the flux, and

Y = meniscus height.

As mentioned earlier, the wetting force measured by the Meniscograph is

$$\sigma = \gamma_{LF}\cos\theta = \sigma_{max} \text{ at equilibrium.}$$

When substituted in Equation 4, this leads to

$$\sin\theta = 1 - \frac{g\ \rho_L-\rho_F}{2}\ \frac{Y^2}{\sigma_{max}}\ \cos\theta$$

which can be found to result in the final expression

$$\theta = \cos^{-1}\frac{2\sigma_{max}KY^2}{\sigma_{max}+K^2Y^4},$$

where K is the constant

$$g\ \frac{\rho_L-\rho_F}{2}.$$

The second method of judging the degree of wetting is using the meniscus height. This is a valid technique as long as the test parameters such as sample size, flux, and test temperature are held constant. The only factor which will then affect the meniscus height is the surface condition of the sample. Although meniscus heights are quantitative data, they are less effective than contact angles since there are no reference values for comparison.

The preceding equation for contact angle can only be used when the specimen is in the form of a flat sheet. This is because of the difference in the ratio of wetting interface length to meniscus surface area for sheet and other sample geometrics (wire). Thus, the meniscus height is the only available information on wetting which can be universally used for all sample shapes.

Test and Data Analysis Procedure

Each sample to be tested was first degreased in trichloroethylene. After being attached to the specimen holder the sample was then immersed in liquid flux to a depth of about 6.4 mm. The sample and holder were then connected to the LVDT over the hot solder pot for approximately 30 seconds to evaporate most of the solvent from the flux which could introduce noise while boiling away during testing.

In addition to the force-time measurements made by the Meniscograph, two optical measurements were taken. Using a Bausch & Lomb stereo microscope with a crosshair eyepiece and a dial depth indicator with a precision of 0.003 mm (0.0001 in.), the immersion depth and meniscus height were measured. This experimental setup is shown in Figure 6. Immersion depth, although not used in any subsequent calculations, was measured as a check on the validity of the quoted immersion depth setting.

The data from each test were then reduced with a Hewlett Packard 9810A programmable calculator with digitizing and plotting capabilities. Output of this system was in the form of a graph of

$$\ln \frac{\sigma_{max}-\sigma}{\sigma_{max}} \text{ versus time.}$$

Regression analysis of the data was performed to force the least squares line through a zero intercept by the use of the expression

$$\text{Slope} = \frac{\sum_{i=1}^{n} x_i y_i}{\sum_{i=1}^{n} x_i^2}.$$

In addition to the plot, test parameters and numerical results such as meniscus height, or calculated contact angle for sheet, were printed on the graph. Figure 7 is an example of the final data output.

Activation energies were also calculated using the programmable calculator system and the reduction technique described earlier. Figure 8 illustrates the plot of

$$\ln \frac{d\sigma}{dt} \text{ versus } \frac{1}{T}$$

which resulted from selected data.

Test and Data Analysis Results

The results from the tests performed are presented in tabular form to provide the reader with a quick comparison of the various factors which could be used to evaluate solderability. Each datum presented is the average value from five tests. In order to judge these various parameters, a few general considerations must be made concerning solderability. The apparent solderability

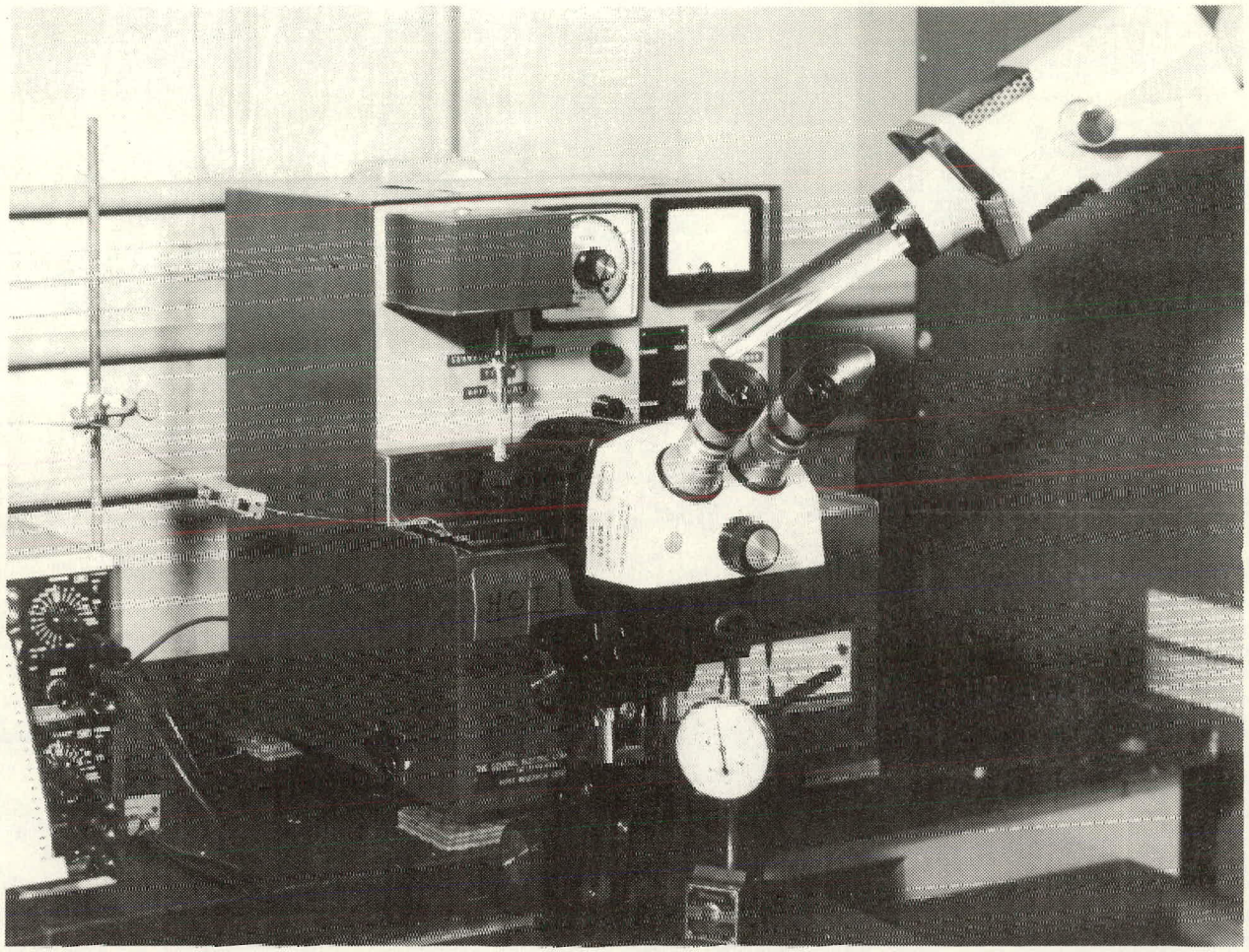

Figure 6. Experimental Setup for Meniscus Height Measurement

of a material will be enhanced as the chemical activity of the flux increases. Thus the fully activated flux (type RA) would be expected to give the best solderability, followed by the mildly activated flux (type RMA), and then the nonactivated flux (type R). Increasing the test temperature, within limits, will also tend to increase the apparent solderability.

Regarding the three materials, it is generally accepted that gold plating affords the best solderability due to its lack of oxides, followed by copper. Nickel, however, is usually considered to be a more difficult material to solder, and requires an activated flux. The various parameters are discussed separately in terms of possible solderability evaluation potential.

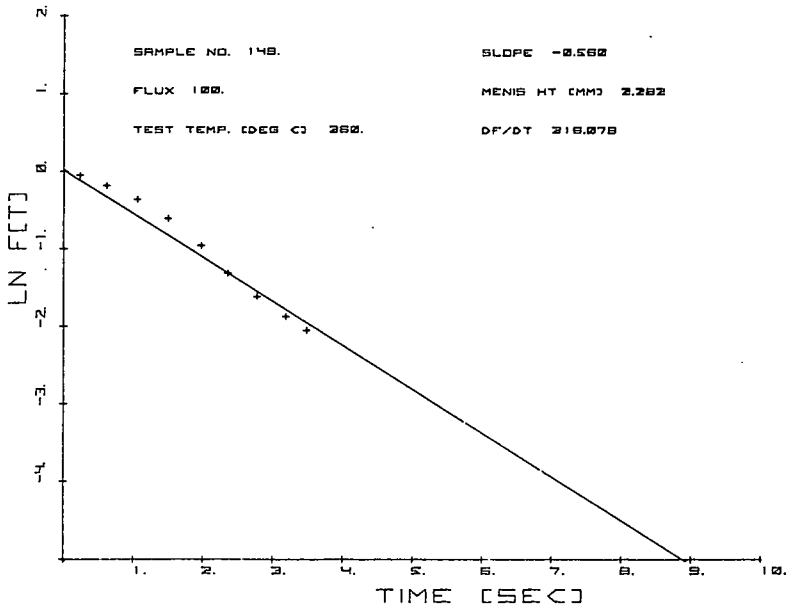

Figure 7. Output Data Used to Evaluate Meniscograph Test Results

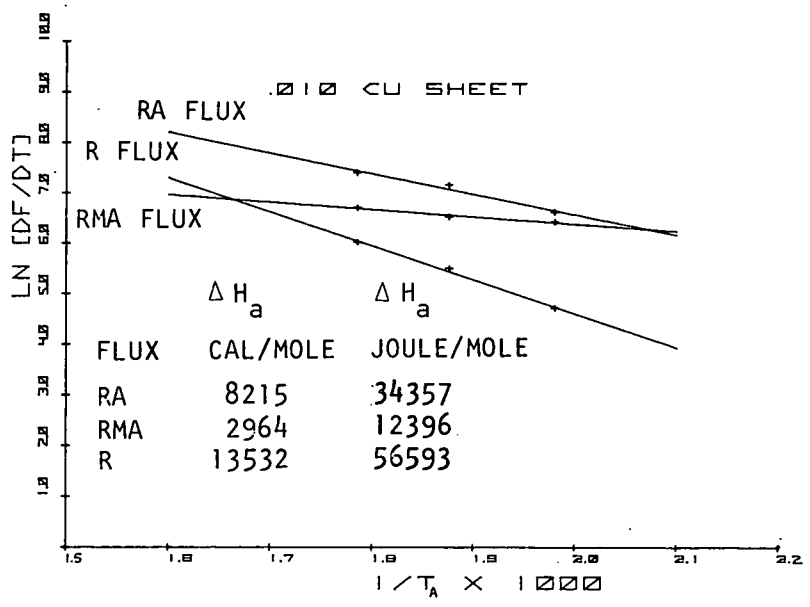

Figure 8. Calculation of Activation Energy From Meniscograph Data

Maximum Wetting Force, σ_{max}

The maximum wetting force data are presented in Table 2. By scanning these data it can be seen that there is little trend in this value as a function of the flux type or test temperature. Values of σ_{max} for nickel samples do, however, seem to be lower than those for the other materials. The conclusion drawn is that this parameter is of very limited, if any, value, and offers no advantage over the familiar spread test.

Wetting Rate, $d\sigma/dt$

In contrast to the maximum wetting force, wetting rate values (Table 3) have definite trends. The wetting rate increases with an increase in both solder temperature and flux activity within specimen material and geometry groups. If the wetting rates for the different materials in the same geometry types are compared, the trends become less straightforward, but at the same time very revealing. Within the 0.3 mm (0.010 in.) thick sheet group, for example, it is evident that the generalized statement that gold plated surfaces exhibit better solderability than copper or nickel surfaces is not completely true. In fact, nickel was found to have the highest wetting rate at increased test temperatures with type RA and RMA fluxes. Within the 0.6 mm (0.022 in.) thick sheet group, the general trends of increased wetting rate with increased flux activity and test temperature are also evident although actual wetting rates are lower than those for the 0.3 mm thick sheet. In this group the nickel sheet exhibits significantly lower wetting rates than the copper. This reversal from the wetting rate data of the 0.3 mm thick sheet may be due to a size effect. The volume of the sample has been essentially doubled which could cause the higher heat capacity and lower thermal conductivity of the nickel to become controlling factors.

In the case of the copper wire, the wetting rates are much higher than for sheet. This supports the speculation of a size effect, since the volume of the wire was much less than that of the sheet. Again, the effects of flux and test temperature are evident. In addition, the wetting rates are significantly higher for the pre-tinned copper wire, as was expected.

A complete discussion and explanation of the test data are not within the scope of this project. Many questions are raised, however, concerning activation temperatures of the fluxes and intrinsic solderability of the materials which might be answered by a more detailed study of these items.

Wetting Angle and Meniscus Height

The calculated wetting angles for the sheet material and the meniscus heights for the wire samples are presented in Tables 4

Table 2. Maximum Wetting Force Values

Sample Type	Size mm (in.)	Flux	Temperature (°C)	Maximum Wetting Force (mN/m)*
Copper Sheet	0.3 (0.01)	RA	232	353
		RMA	232	381
		R	232	373
		RA	260	375
		RMA	260	371
		R	260	374
		RA	287	379
		RMA	287	361
Copper Sheet	0.3 (0.01)	R	287	447
Gold Plated Copper Sheet	0.3 (0.01)	RA	232	356
		RMA	232	377
		R	232	415
		RA	260	375
		RMA	260	389
		R	260	426
		RA	287	363
Gold Plated		RMA	287	382
Copper Sheet	0.3 (0.01)	R	287	393
Nickel Sheet	0.3 (0.01)	RA	232	345
		RMA	232	314
		R	232	NA**
		RA	260	330
		RMA	260	310
		R	260	NA
		RA	287	333
		RMA	287	272
Nickel Sheet	0.3 (0.01)	R	287	NA
Copper Sheet	0.6 (0.022)	RA	232	338
		RMA	232	356
		R	232	350
		RA	260	342
		RMA	260	367
		R	260	350
		RA	287	360
		RMA	287	421
Copper Sheet	0.6 (0.022)	R	287	356

Table 2 Continued. Maximum Wetting Force Values

Sample Type	Size mm (in.)	Flux	Temperature (°C)	Maximum Wetting Force (mN/m)*
Copper Sheet	0.6 (0.022)	RA	232	338
		RMA	232	356
		R	232	350
		RA	260	342
		RMA	260	367
		R	260	350
		RA	287	360
		RMA	287	421
Copper Sheet	0.6 (0.022)	R	287	356
Nickel Sheet	0.5 (0.0215)	RA	232	388
		RMA	232	NA
		R	232	NA
		RA	260	324
		RMA	260	NA
		R	260	NA
		RA	287	327
		RMA	287	NA
Nickel Sheet	0.5 (0.0215)	R	287	NA
Copper Wire	0.8 (0.03)	RA	232	373
		RMA	232	388
		R	232	395
		RA	260	374
		RMA	260	394
		R	260	399
		RA	287	362
		RMA	287	370
Copper Wire	0.8 (0.03)	R	287	379
Pretinned Copper Wire	0.8 (0.03)	RA	232	370
		RMA	232	372
		R	232	392
		RA	260	352
		RMA	260	342
		R	260	418
		RA	287	361
		RMA	287	386
Pretinned Copper Wire	0.8 (0.03)	R	287	397

*1 mN/m = 1 dyne/cm
**Not Available

Table 3. Wetting Rate Values

Sample Type	Size mm (in.)	Flux	Temperature (°C)	Wetting Rate, dσ/dt (mN/m/sec)
Copper Sheet	0.3 (0.01)	RA	232	766
		RMA	232	629
		R	232	113
		RA	260	1326
		RMA	260	704
		R	260	249
		RA	287	1700
		RMA	287	843
Copper Sheet	0.3 (0.01)	R	287	422
Gold Plated Copper Sheet	0.3 (0.01)	RA	232	1077
		RMA	232	608
		R	232	144
		RA	260	1230
		RMA	260	684
		R	260	350
		RA	287	1235
Gold Plated		RMA	287	974
Copper Sheet	0.3 (0.01)	R	287	929
Nickel Sheet	0.3 (0.01)	RA	232	924
		RMA	232	724
		R	232	0
		RA	260	2318
		RMA	260	1294
		R	260	0
		RA	287	3412
		RMA	287	1060
Nickel Sheet	0.3 (0.01)	R	287	0
Copper Sheet	0.6 (0.022)	RA	232	734
		RMA	232	323
		R	232	154
		RA	260	987
		RMA	260	628
		R	260	389
		RA	287	1036
		RMA	287	793
Copper Sheet	0.6 (0.022)	R	287	470

Table 3 Continued. Wetting Rate Values

Sample Type	Size mm (in.)	Flux	Temperature (°C)	Wetting Rate, dσ/dt (mN/m/sec)
Nickel Sheet	0.5 (0.0215)	RA	232	113
		RMA	232	0
		R	232	0
		RA	260	196
		RMA	260	0
		R	260	0
		RA	287	246
		RMA	287	0
Nickel Sheet	0.5 (0.0215)	R	287	0
Copper Wire	0.8 (0.03)	RA	232	2728
		RMA	232	370
		R	232	43
		RA	260	2824
		RMA	260	1065
		R	260	180
		RA	287	3064
		RMA	287	2453
Copper Wire	0.8 (0.03)	R	287	621
Pretinned Copper Wire	0.8 (0.03)	RA	232	5181
		RMA	232	2689
		R	232	869
		RA	260	4929
		RMA	260	3082
		R	260	1288
		RA	287	6644
		RMA	287	3678
Pretinned Copper Wire	0.8 (0.03)	R	287	2563

and 5. Although the trends in wetting angle for the sheet material are the same as for wetting rates, the trends appear to be less definite. An examination of the meniscus height values for the wire exhibit no trends. Further investigation into the experimental technique used to measure meniscus height has indicated that there was in fact some margin for introduced errors which could be the cause of the questionable results.

Table 4. Wetting Angle Values

Sample Type	Size mm (in.)	Flux	Temperature (°C)	Wetting Angle (Degrees)
Copper Sheet	0.3 (0.01)	RA	232	31
		RMA	232	34
		R	232	41
		RA	260	33
		RMA	260	49
		R	260	37
		RA	287	20
		RMA	287	34
Copper Sheet	0.3 (0.01)	R	287	41
Gold Plated Copper Sheet	0.3 (0.01)	RA	232	19
		RMA	232	26
		R	232	33
		RA	260	15
		RMA	260	22
		R	260	24
		RA	287	18
Gold Plated Copper Sheet	0.3 (0.01)	RMA	287	15
		R	287	17
Nickel Sheet	0.3 (0.01)	RA	232	20
		RMA	232	40
		R	232	NA*
		RA	260	31
		RMA	260	46
		R	260	NA
		RA	287	30
		RMA	287	38
Nickel Sheet	0.3 (0.01)	R	287	NA
Copper Sheet	0.6 (0.022)	RA	232	29
		RMA	232	38
		R	232	34
		RA	260	23
		RMA	260	32
		R	260	34
		RA	287	40
		RMA	287	46
Copper Sheet	0.6 (0.022)	R	287	31

Table 4 Continued. Wetting Angle Values

Sample Type	Size mm (in.)	Flux	Temperature (°C)	Wetting Angle (Degrees)
Nickel Sheet	0.5 (0.0215)	RA	232	28
		RMA	232	NA
		R	232	NA
		RA	260	29
		RMA	260	NA
		R	260	NA
		RA	287	32
		RMA	287	NA
Nickel Sheet	0.5 (0.0215)	R	287	NA

*NA indicates no wetting occurred

ACCOMPLISHMENTS

Solderability test procedures and data reduction techniques applicable to the Meniscograph have been developed which permit the calculation of actual wetting rates from the raw force-time output data. The results were found to provide a useful comparison of the solderability of various materials as well as information regarding flux, temperature, and size effects. Wetting angle calculations were also found to be useful indicators of solderability. Errors in the measurement of meniscus height must be minimized, however, if this parameter is to be fully utilized.

In addition to being able to provide data directly related to the wetting phenomenon, the Meniscograph offers the unique advantage of being able to test samples of almost any configuration. The need for making test samples which significantly differ from actual parts in order to accommodate the test method is, therefore, substantially reduced.

FUTURE WORK

Efforts are underway to construct equipment for meniscus height measurement which will minimize errors identified in this study. In addition, an expression relating wetting angle to meniscus height for wire is currently being derived.

Table 5. Meniscus Height Values

Sample Type	Size mm (in.)	Flux	Temperature (°C)	Meniscus Height mm (in.)
Copper Wire	0.8 (0.03)	RA	287	0.896 (0.0352)
		RMA	287	0.925 (0.0364)
		R	287	0.876 (0.0345)
		RA	232	0.901 (0.0354)
		RMA	232	0.872 (0.0343)
		R	232	0.902 (0.0355)
		RA	260	0.877 (0.0345)
		RMA	260	0.900 (0.0354)
Copper Wire	0.8 (0.03)	R	260	0.922 (0.0362)
Pre-tinned Copper Wire	0.8 (0.03)	RA	232	0.864 (0.340)
		RMA	232	0.975 (0.0383)
		R	232	1.070 (0.0421)
		RA	260	0.880 (0.346)
		RMA	260	0.995 (0.0391)
		R	260	0.961 (0.0378)
		RA	287	0.902 (0.0355)
Pre-tinned Copper Wire	0.8 (0.03)	RMA	287	0.940 (0.0370)
		R	287	0.965 (0.0379)

A computer program is being written which will allow the data reduction by the Bendix scientific computer via a graphics terminal. This will provide a much greater data reduction capability should future work indicate program modifications or additions to be necessary.

Future test programs involving the Meniscograph could include soldering temperature optimization, solder alloy selection and characterization, quality control functions, and further investigation of the wetting phenomenon itself. It is also suspected that, with slight modification the Meniscograph could be utilized as a supplemental test to the water drop test used to evaluate surface cleanliness.

REFERENCES

[1]J. L. Jellison and others, "Statistical Interpretation of Meniscograph Solderability Tests," *Transactions, Parts, Hybrids, and Packaging*, Volume 12, Number 2: IEEE, June, 1972.

[2]A. W. Adamson, *Physical Chemistry of Surfaces*. New York: John Wiley & Sons, 1967.

[3]A. J. Mayhew and F. R. Wicks, "Solderability and Contact Angle," *Proceedings International Nepcon III*, 1971.

[4]J. F. Shipley, "Influence of Flux, Substrate, and Solder Composition on Solder Wetting," *Welding Research Supplement*, 1975.

BIBLIOGRAPHY

Adamson, A. W., *Physical Chemistry of Surfaces*. New York: John Wiley & Sons, 1967.

Che, T. Y., "A Hydrostatic Model of Solder Fillets," *Welding Research Supplement*, January, 1975.

Circuits Manufacturing, July, 1973, "The Meniscograph: A Method of Solderability Measurement."

Jellison, J. L. and others, "Statistical Interpretation of Meniscograph Solderability Tests," *Transactions, Parts, Hybrids, and Packaging*, Volume 12, Number 2: IEEE, June, 1972.

Mayhew, A. J. and F. R. Wicks, "Solderability and Contact Angle," *Proceedings International Nepcon III*, 1971.

Orr, F. M. and others, "Pendular Rings Between Solids: Meniscus Properties and Capillary Force," *Journal of Fluid Mechanics*, Volume 67, Part 4, 1975.

Pentanelli, G. P., "Measurement of the Solderability of Thick-Film Circuits, Relationship Between Solder Strength and a Solderability Test," *Solder State Technology*, October, 1975.

Shipley, J. F., "Influence of Flux, Substrate, and Solder Composition on Solder Wetting," *Welding Research Supplement*, 1975.

TenDuis, J. A. and E. van der Meulen, "Measurement of the Solderability of Components," *Philips Technical Review*, Volume 28, Number 18, 1967.

Wallis, D. R., "Assessment of Solderability," *The Metallurgist and Materials Technologist*, January, 1974.

DISTRIBUTION

	Copy
R. Bulcock, ERDA-KCAO	1
V. C. Vespe, ERDA-ALO	2
J. A. Freed, LASL	3
S. J. Buginas, LLL	4
R. J. Hersey, LLL	5
F. J. Huegel, LLL	6
H. M. Brinkmeier, Monsanto	7
H. M. Barnett, SLA	8
J. F. Dal Porto, SLA	9
J. L. Jellison, SLA	10
C. W. Jennings, SLA	11
D. R. Adolphson, SLL	12
A. D. Andrade, SLL	13
J. W. Dini, SLL	14
J. D. Corey, D/554, BD50	15-16
L. Stratton, D/552, 2C44	17-19
R. F. Cell, D/755, 1A42	20
R. P. Frohmberg, D/800	21
R. L. Comstock, D/814, 2C43	22
W. H. Deterding, D/814, 2C43	23
D. M. Jarboe, D/814, 2C43	24-28
H. B. Pressly, D/814, 2C43	29
R. L. Sadler, D/814, 2C43	30
D. L. Stoltz, D/814, 2C43	31
B. W. Landes, D/821, 2A36	32
R. J. Setter, D/821, 2A36	33
A. O. Bendure, D/842, MD40	34
J. S. Bosnak, D/842, MD40	35
S. Landers, D/842, MD40	36
J. A. Peters, D/842, MD40	37
D. D. Peterson, D/842, MD40	38
T. A. Wiley, D/842, MD40	39
R. E. Schmidt, D/844, BW31	40
D. A. Cummins, D/845, MF39	41
R. C. Douglass, D/845, MF39	42
R. J. Powell, D/845, MF39	43
W. R. Sprague, D/845, MF39	44
R. A. Wilson, D/845, MF39	45
H. F. Darbyshire, D/862, MA40	46
M. Gray, D/862, MA40	47
B. T. Gregg, D/862, MA40	48
J. C. McCoy, D/862, MA40	49
R. E. Kessler, D/865, 2C40	50

THIS PAGE IS UNCLASSIFIED

BDX-613-1706 PDO 6989288

SOLDERABILITY TEST DEVELOPMENT, D. M. Jarboe, D/814, UNCLAS Final, October 1977.

Operating procedures and data reduction techniques applicable to a General Electric Company, Limited, Meniscograph were developed. The information provides a means of directly correlating solderability with the physical phenomenon of wetting.

MECHANICAL: Solderability

SOLDERABILITY TEST DEVELOPMENT, D. M. Jarboe, D/814, UNCLAS Final, PDO 6989288, BDX-613-1706, October 1977.

Operating procedures and data reduction techniques applicable to a General Electric Company, Limited, Meniscograph were developed. The information provides a means of directly correlating solderability with the physical phenomenon of wetting.

SOLDERABILITY TEST DEVELOPMENT, D. M. Jarboe, D/814, UNCLAS Final, PDO 6989288, BDX-613-1706, October 1977.

Operating procedures and data reduction techniques applicable to a General Electric Company, Limited, Meniscograph were developed. The information provides a means of directly correlating solderability with the physical phenomenon of wetting.